Cerium removal by activated carbon derived from palm kernel shell

Chee-Heong Ooi[1], Akane Ito[2], Tsubasa Otake[2], Fei-Yee Yeoh[1]*

[1]*School of Materials & Mineral Resources Engineering, Universiti Sains Malaysia, Transkrian Engineering Campus, 14300 Nibong Tebal, Penang, Malaysia*
[2]*Division of Sustainable Resources Engineering, Faculty of Engineering, Hokkaido University, Kita 13 Nishi 8, Kita-ku, Sapporo, Hokkaido 060-0828, Japan*

*Corresponding author; Tel: (+60) 4-5996175; Fax: (+60) 4-5991011; E-mail: feiyee@usm.my, yeoh.usm@gmail.com

Received: 05 September 2016, Revised: 06 October 2016 and Accepted: 22 November 2016

DOI: 10.5185/amlett.2017.7061
www.vbripress.com/aml

Abstract

Palm kernel shell (PKS) was utilized as a precursor for the preparation of activated carbon (AC) via different carbonization temperatures and carbon dioxide gas activation processes. The physical and chemical properties of the AC samples were studied by TGA, nitrogen adsorption analysis and SEM. The results show that the AC sample with BET surface area up to 622 $m^2 g^{-1}$ and total pore volume of 0.297 $cm^3 g^{-1}$ with narrow pore size of 1.2 nm were obtained. The SEM shows that more pores were revealed on the surface of AC after the carbonization and activation processes. The AC samples carbonized at 500 and 600 °C (CA-500 and CA-600) exhibited higher Ce removal percentage (99.94 %) than that of the other samples. Higher BET surface area of the CA-500 and CA-600 samples resulted in slightly more Ce ions to be adsorbed and precipitated compared to that of other samples. The result indicates that high pH value and BET surface area of AC sample has a rather strong influence on Ce removal. AC samples show excellent Ce removal capacity, thereby; the results suggest that the PKS-based AC could be a promising adsorbent for the cerium removal application. Copyright © 2016 VBRI Press.

Keywords: Palm kernel shell, activated carbon, BET surface area, pore size distribution, cerium removal.

Introduction

Cerium (Ce) is an abundant and cheap rare earth element (REE). It exists as both stable and radioactive isotopes. The REE is commonly used in catalyst support, polishing powders, superalloys, electronics components, artistic glasses, optic filters and steel modifiers **[1, 2]**. Inhalation and long-term exposure to the radioactive REE may cause lung cancer **[3]**. Reports shows that numerous cases of workers suffered from harmful lung disease such as interstitial lung disease and pneumoconiosis are associated with accumulation of Ce in the lungs after prolonged occupational exposure to Ce fumes or dust **[4]**. Consumption of water contaminated with Ce can be a threat to liver when it accumulates in the human body **[5]**.

Therefore, removal of the Ce from waste water prior to environmental discharge is an essential step to ensure the safety and quality of lives. The removal of REE can be done via Ce precipitation and adsorption process. Activated carbon (AC) can be utilized for the effective REE removal process due to its extraordinary pore characteristics. AC has large surface area, high porosity and high adsorption capacity **[6, 7]**. Saleem and co-workers utilized activated charcoal for selective adsorption of Ce from aqueous electrolyte solutions **[8]**. Sodium lauryl sulfate (NaLS) was used to modify the AC surface and apply for adsorptive removal of Ce from the aqueous solutions **[9]**. These studies indicated the possibility of applying AC as an efficient adsorbent for the Ce removal process. The widespread of the AC is limited due to the expensive conventional raw materials. Greater cost is needed to produce the AC with outstanding pore characteristics and adsorption capacity **[10]**. Agricultural and industrial biomass are the perfect raw materials for the production of low cost and bio-friendly adsorbents since they are available in great quantities with consistent supply, inexpensive and involve very little processing **[11]**.

Every year, Malaysia produces about 39 % of the total world's supply of palm oil **[12]**. The large-scale palm oil production has resulted in huge amount of biomass generated annually, including palm kernel shell (PKS), which requires an effective disposal solution. PKS has very low commercial value and is usually used as solid fuel in boiler to generate steam. However, the poor combustion characteristic of PKS leads to smoke emission, serious air and environmental pollutions. In contrast, due to its constant availability, relatively high density and carbon content **[13]**, PKS is an ideal raw material that could be value-added into AC instead of being treated as an agricultural waste. In addition, the AC produced from PKS **[14]** has high BET surface area comparable to the conventional coal based AC **[15]**. At present, the study on Ce removal via adsorption by biomass-based AC is very limited. The conversion of PKS into AC could provide effective solution for the Ce removal process and contribute to the wealth generation for nation (conversion of PKS biomass into porous adsorbent). The PKS-based AC would act as efficient adsorbent for Ce removal due to its good pore characteristics. In this study, the PKS-based AC was prepared via carbonization and followed by carbon dioxide (CO_2) activation. The effect of carbonization temperature on the pore characteristics and Ce removal capacity of the AC samples were investigated.

Experimental

Material synthesis

The PKS used in this study was obtained from United Palm Oil Mill, Nibong Tebal, Malaysia. The PKS was first cleaned with 5 % nitric acid and dried in oven. The clean PKS was carbonized at different temperatures (400, 500 and 600 ºC) without any external gas supply. The carbonized PKS was then treated with sulfuric acid (H_2SO_4) at a 0.75:1 (acid-to-PKS) ratio. For activation, the sample was heated to 900 ºC under a constant nitrogen (N_2) gas flow (100 ml min^{-1}). At 900 ºC, the N_2 gas supply was turned off and CO_2 gas (100 ml min^{-1}) was purged into furnace (OTF-1200X tube furnace) for one hour. Upon completion of activation process, the CO_2 gas supply was turned off and switched back to N_2 gas flow. The final samples carbonized at 400, 500 and 600 ºC are denoted as CA-400, CA-500 and CA-600, respectively.

Characterizations

The thermal behaviors of PKS were analyzed by using Netzsch-Geratebau GmbH-STA 409 PC Luxx simultaneous thermal analyzer. N_2 adsorption instrument (Quantachrome autosorb iQ) was used to measure the physisorption of the samples towards N_2 at -196 ºC. The Specific surface areas of these samples were calculated from nitrogen adsorption results by applying Brunauer-Emmett-Teller (BET) model. The pore size distribution (PSD) of the AC samples was obtained by employing the Density Functional Theory (DFT). The total pore volumes were determined at relative pressure of 0.99. Surface morphology of the AC samples was investigated using Zeiss Supra 35VP scanning electron microscopy (SEM).

Cerium removal

Standard Ce solutions at different concentration (0.01, 0.05, 0.1. 0.5, 1.0, 5.0 and 10 ppb) was prepared. 10 ppb Ce standard solution was prepared by adding 0.05 mL of Ce solution (10 ppm) into 50 mL volumetric flask that contained 49.95 mL ultrapure water. The 10 ppb solution was diluted to prepare Ce standard solutions at different concentrations. The Ce standards solutions were analyzed via an inductively coupled plasma-mass spectrometry (Thermo Scientific iCAP Q ICP-MS) to develop the standard calibration curve for Ce solutions.

500 mL of Ce solution (500 ppb) was prepared by adding 0.435 g of Sodium nitrate ($NaNO_3$) and 0.250 mL of Ce standard solution (1000 ppm) into 500 mL volumetric flask that contained ultrapure water. The mixture in volumetric flask was then inverted repeatedly to ensure that the Ce solution and ultrapure water were mixed homogeneously. The Ce removal study was carried out by adding 0.4 g of AC sample into 40 mL of Ce solution (500 ppb) in a centrifuge tube. The solution was prepared at pH 4 as the optimum condition for Ce removal process to occur **[8]**. A pH meter was used to monitor the pH changes in Ce solutions before and after the Ce removal process. The centrifuge tubes which contained mixture of AC and Ce solution were then placed on rotary shaker (80 rpm). The shaking process was stopped after 24 hours and the Ce solution was sampled using a syringe filter. The Ce solutions were analyzed via ICP-MS and compared to standard calibration curve to determine the amount of Ce removal.

Results and discussion

Fig. 1 shows the thermogravimetric curves of PKS during pyrolysis and combustion that carried out in N_2 and oxygen (O_2) gas atmospheres respectively. The thermal decomposition of PKS during the pyrolysis can be classified into three main stages such as moisture evaporation, major devolatilization and continuous minor devolatilization **[16]**. About 5.03 wt % of weight loss occurred at temperature below 150 ºC. This weight loss was due to the moisture evaporation **[17]**. The main devolatilization happened at the temperature range from 200 to 400 ºC with a weight loss of 45.64 wt %. This devolatilization was attributed to the thermal decomposition of hemicelluloses and cellulose **[18]**. A gradual weight loss was observed at the range from 400 to 900 ºC and it was caused by the subsequent thermal decomposition of lignin **[19]**. The thermal of behavior of the PKS in the present study shows agreement with the pyrolyzed PKS reported by Kim and co-workers **[20]**.

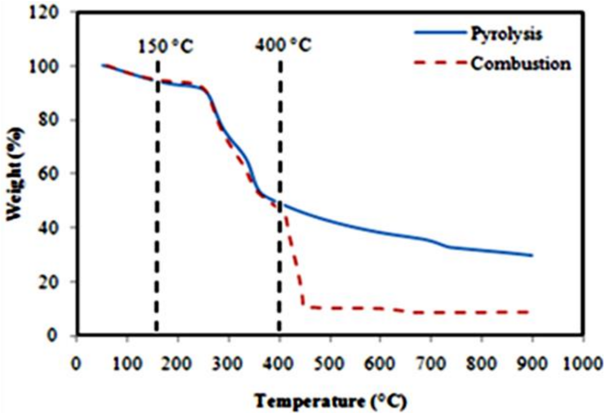

Fig. 1. Thermogravimetric curves of PKS during pyrolysis and combustion.

Similar thermal decomposition profile was shown by combustion of PKS. The initial weight loss (4.53 wt %) at temperature below 150 ºC was due to the moisture evaporation. The subsequent thermal degradations was attributed to the oxidation of volatile products and followed by the char oxidation **[21]**. The oxidative degradation for the PKS occurred at 150 to 420 ºC. A drastic weight loss of 58.48 wt % in this range was caused by the decomposition of hemicelluloses, cellulose and the partial decomposition of lignin **[22]**. After the devolatilization of cellulosic materials in PKS at 420 ºC, the porosity in char increased and oxygen diffused easily into char to react with the carbon residual **[23]**. Hence, this process resulted in a drastic weight loss which was not observed in the PKS pyrolyzed in N_2 atmosphere. The difference in weight loss between pyrolyzed and a combusted PKS sample was equivalent to the amount of carbon residual decomposed during the char combustion. Based on the thermogravimetric curves of PKS, AC samples were carbonized at three different temperatures (400, 500 and 600 ºC). This is the temperature range where thermal degradation of volatile matters into simple carbon structure occurs that contributes to the fixed carbon content and development of porous structure.

The N_2 adsorption and desorption isotherms of the AC samples are shown in **Fig. 2**. The isotherms for the AC samples pertain to type I isotherm according to the International Union of Pure and Applied Chemistry (IUPAC) classification. The amount of N_2 uptake for the AC samples increased rapidly up to relative pressure 0.02. The large amount of N_2 uptake at the extremely low relative pressure shows that the PKS-based AC samples mainly consist of micropores **[24]**. The N_2 uptake increased with an increase in carbonization temperature of the AC samples, suggesting a better micropores development at higher carbonization temperature. Thus, it is obvious that high carbonization temperature could result in the production of AC with great porosity due to burn off of more organic volatile matters **[25]**. The adsorption capacity of PKS-based is largely depends on the presence of micropores volume. Hence, high carbonization temperature could produce porous PKS-based AC with excellent adsorption capacity.

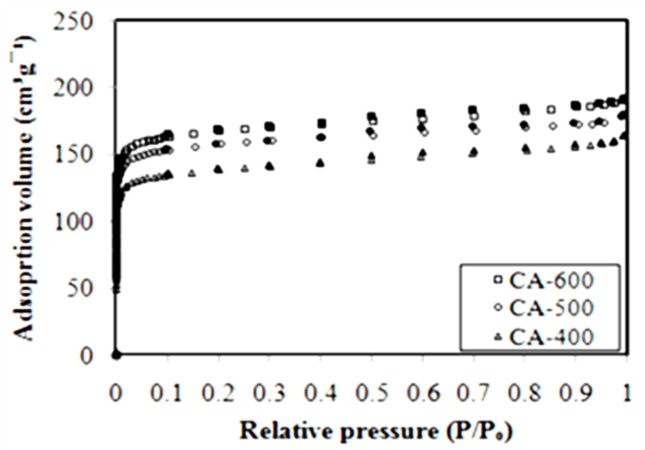

Fig. 2. Adsorption and desorption isotherms of N_2 by PKS-based AC samples.

Fig. 3 shows the pore size distribution of (PSD) of AC samples carbonized at different temperature. The AC samples exhibit three major peaks in the microporous range with respective widths of 1.2, 1.5 and 1.9 nm, respectively. There are other small peaks distributed across the mesoporous range (2nm < pore width < 50 nm). All the AC samples show the highest peak with a narrow PSD at the pore width of 1.2 nm. This result indicates that the AC samples derived from PKS contained large amount of microporosity with mode pore size of 1.2 nm.

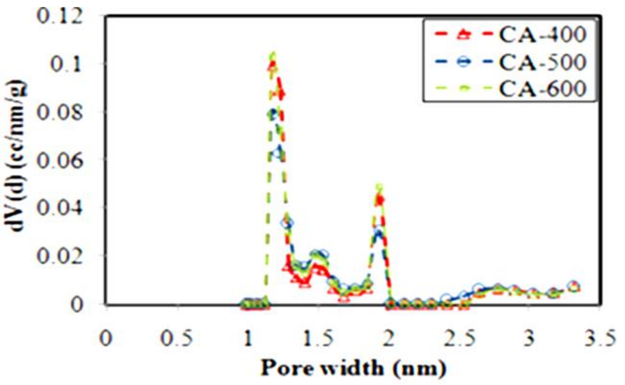

Fig. 3. Pore size distributions of PKS-based AC samples.

Table 1. Pore characteristics of the AC samples prepared at different carbonization temperature.

Sample	Burn-off (%)	BET surface area ($m^2 g^{-1}$)	Total pore volume ($cm^3 g^{-1}$)
CA-400	60.6	541	0.25
CA-500	72.2	615	0.28
CA-600	74.8	622	0.30

The pore characteristics of the PKS-based AC samples prepared at different carbonization temperature are presented in **Table 1**. The burn-off, that is an preliminary indication of the degree of pore development (burn off of volatile organic matters from precursor), is 74.8 % for CA-600, higher than that of CA-500 (72.2 %) and CA-400 (60.6 %). The BET surface areas for CA-400, CA-500 and CA-600 samples are 541, 615 and 622 m^2g^{-1}, respectively. The BET surface areas of the AC samples increased with the increase of carbonization temperatures. The total pore volume for CA-600 (0.30 cm^3g^{-1}) is higher than that of CA-500 (0.28 cm^3g^{-1}) and CA-400 (0.25 cm^3g^{-1}), showing the similar trend with the BET surface area. When the carbonization temperatures increased, more volatile organic matters (which caused blockage in carbon structures) were eliminated and eventually enhanced the pore development during the activation **[26]**. The BET surface areas of the AC samples produced in the present study is comparable to AC derived from conventional coconut shell (524 m^2 g^{-1}) and coal (550 – 790 m^2 g^{-1}) **[27, 28]**. The results show that the PKS-based AC exhibits good pore characteristics and comparable to conventional precursors. The PKS-based AC is more bio-friendlier than the conventional precursors and could be used as an efficient adsorbent for Ce removal application.

Fig. 4 shows the SEM images of the PKS and CA-600 that were taken at 500X magnification. An uneven surface and small pores were observed on the PKS surface. Some of the pores in PKS were blocked by organic matters. However, the organic matters which caused the blockage in the pores of PKS were burnt off after carbonization and activation processes (**Fig. 4 (b)**).

The CA-600 sample has an uneven external surface and numerous large pores were found. CA-400 and CA-500 samples also exhibited similar porous structure as shown by the CA-600 sample. Uneven external surfaces with the presence of enormous amount of pores were found on the samples. The pores on the surface of PKS-based AC would act as connecting channels to enable adsorbate molecules diffusing easily into the internal micropores during the adsorption process.

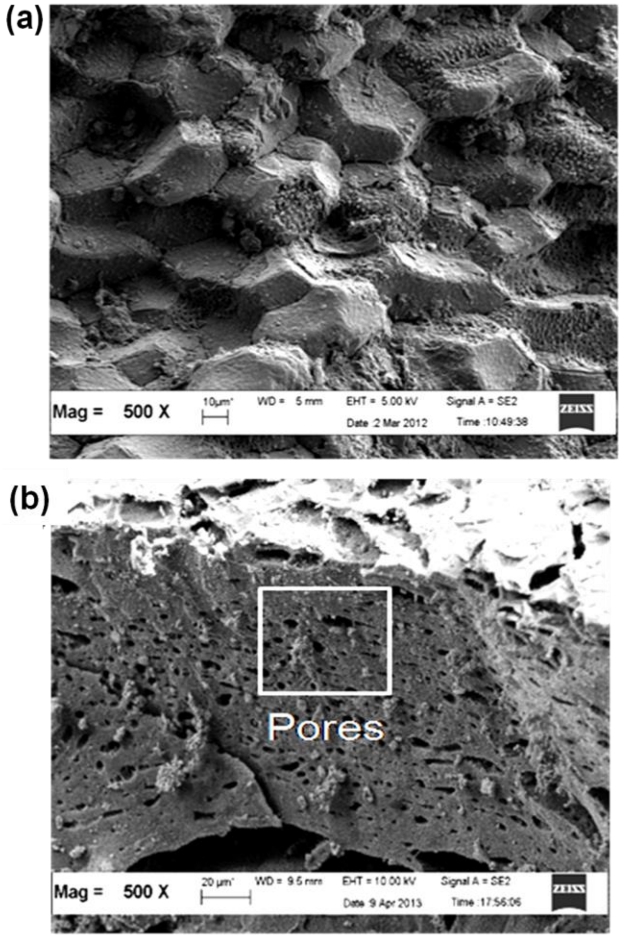

Fig. 4. SEM images of the (a) PKS and (b) CA-600 samples.

The change in pH could lead to the precipitation of Ce and affect the amount of Ce removal **[8].** The present study investigates the effect on the amount Ce ions precipitated due to increasing pH. **Fig. 5** shows the concentration of Ce solutions as a function of pH. The initial concentration of Ce solution at pH 4 was 516.060 ppb and the concentration of the Ce solution decreased as pH increasing. At pH above 4, the precipitation starts to take place in aqueous solution and decrease in the concentration of Ce solutions is resulted. A drastic decrease in concentration of Ce solution happened when the pH is above 8. The amount of Ce ions precipitated increased from 15.27 ppb at pH 6 to 465.83 ppb at pH 10 (Concentration at pH 10 is 465.827 ppb). The result shows that increase in pH would cause the decrease in concentration of Ce solution and eventually increased the amount of Ce removal.

Ce removal study was carried out using the PKS-based AC samples. The Ce removal capacities of the AC samples were compared to commercial AC and zeolites samples. The pH changes in Ce solutions added with PKS-based AC, commercial AC and zeolites are shown in **Fig. 6**.

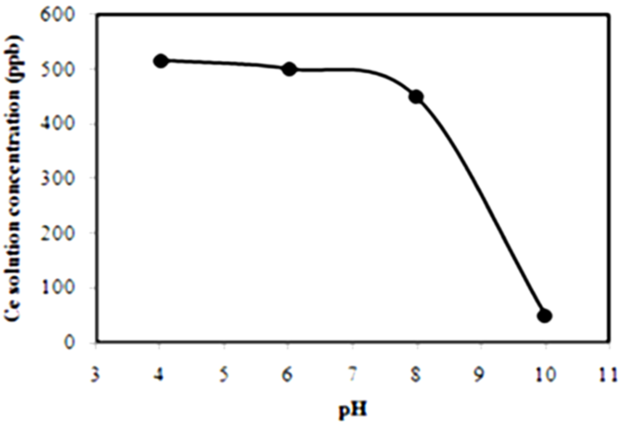

Fig. 5. Change in concentration of Ce solutions at different pH.

The pH values for Ce solutions added with AC samples ranged from 9.2 to 11, while the pH for Ce solution added with zeolites was pH 4.6. The CA-400 shows relatively higher pH values than that of the other AC samples and this possibility due to the difference in carbonization temperature. More inorganic matters will be burnt off and formed ash when PKS was carbonized at higher temperature. The ash formed contains CaO **[29]** and could result in increase in pH value. The ash content will be washed and removed prior to activation process. Thus, more ash content will be removed when PKS-based AC sample carbonized at higher temperature and eventually exhibited lower pH value. Increase in the Ce solution pH from initial pH 4 is due to the surface alkalinity of AC samples, suggesting that the PKS-based AC samples are rather basic. The change in pH values influences the capacity of Ce removal by the AC samples. According to the report by Saleem and co-workers **[8]**, the concentration of Ce in the solution was greatly reduced when the pH increased bringing about better Ce removal through precipitation. The increase in pH caused the precipitation of Ce ions and eventually reduced the concentration of Ce solution.

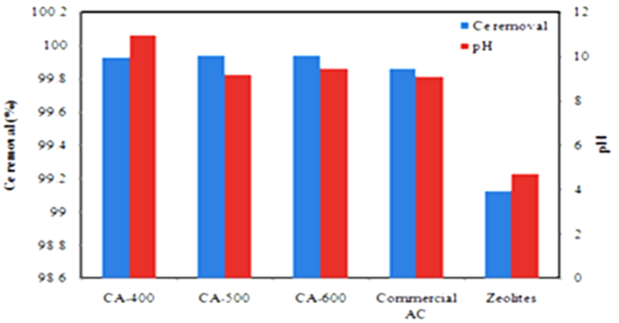

Fig. 6. Percentage of Ce removal by PKS-based AC, commercial AC and zeolites.

The best Ce removal is shown by CA-600 (99.94 %) and CA-500 (99.94 %) followed by CA-400 (99.93 %), commercial AC (99.86 %) and zeolites (99.13 %) as shown in **Fig. 6**. Higher BET surface areas of CA-600 and CA-500 caused slightly more Ce ions to be adsorbed and precipitated compared to that of other samples. During the adsorption, Ce ions migrate from the Ce solution into the pores of the AC via diffusion process and subsequently adsorbed on the pore walls and possibly precipitated due to pH changes. Thus, more Ce ions could be adsorbed on the internal surface of the AC sample with larger BET surface area. The result also illustrates that high pH value and BET surface area of AC sample has a rather strong influence on Ce removal.

Table 2 shows the percentage of Ce removal by various adsorbents. The percentage of Ce removal by the PKS-based AC is comparable to other type of adsorbents. The results indicated that PKS-based AC could potentially be utilized as an efficient adsorbent for the Ce removal process.

Table 2. Percentage of Ce removal by various adsorbents

Adsorbent	Percentage of Ce removal (%)	Reference
PKS-based AC	99.94	This work
Carboxylate-rich wheat straw	90.00	[30]
Grapefruit peel	95.00	[31]
Monosodium glutamate functionalized chitosan beads	99.70	[32]
SBA-15 mesoporous silica	99.63	[33]

Conclusion

The results reveal the effective PKS disposal alternative by converting it into porous AC via carbonization and CO_2 activation processes. Increase in carbonization temperature was found to improve the AC pore development. The SEM shows that many pores were formed on the surface of AC after the carbonization and activation processes. The pores on the AC surface would act as connecting channel to enable more Ce ions adsorbed onto the internal micropores. CA-600 and CA-500 with higher BET surface areas show better Ce removal percentage than CA-400, commercial AC and zeolites samples. The PKS-based AC samples could be utilized as a bio-friendly and efficient adsorbent for Ce removal up to 99.94 % effectiveness.

Acknowledgements

The authors would like to thank Universiti Sains Malaysia (USM), MOE, MOSTI, Hokkaido University and JASSO for the financial support provided for this research.

References

1. Sert, S.; Kütahyali, C.; İnan, S.; Talip, Z.; Çetinkaya, B.; Eral, M.; *Hydrometallurgy*, **2008**, *90*, 13.
2. Palmieri, M. C.; Garcia, O.; Melnikov, P.; *Process Biochem.*, **2000**, *36*, 441.
3. Cember, H.; Stemmer, K.; *Health Phys.*, **1964**, *10*, 43.
4. Yoon, H.; Moon, H.; Park, S.; Song, J.; Lim, Y.; Kohyama, N.; *Thorax*, **2005**, *60*, 701.
5. Schubert, D.; Dargusch, R.; Raitano, J.; Chan, S. W.; *Biochem. Biophys. Res. Commun.*, **2006**, *342*, 86.
6. Matos, J.; Nahas, C.; Rojas, L.; Rosales, M.; *J. Hazard. Mater.*, **2011**, *196*, 360.
7. Phan, N. H.; Rio, S.; Faur, C.; Coq, L. Le; Cloirec, P. L.; Nguyen, T. H.; *Carbon*, **2006**, *44*, 2569.
8. Saleem, M.; Afzal, M.; Qadeer, R.; Hanif, J.; *J. Radioanal. Nucl. Chem.*, **1993**, *172*, 257.
9. Mahmoud, M. R.; Sharaf El-deen, G. E.; Soliman, M. A.; *Ann. Nucl. Energy*, **2014**, *72*, 134.
10. Babel, S.; Kurniawan, T. A.; *J. Hazard. Mater.*, **2003**, *97*, 219.
11. Crini, G.; *Bioresour. Technol.*, **2006**, *97*, 1061.
12. Johari, A.; Nyakuma, B. B.; Nor, S. H. M.; Mat, R.; Hashim, H.; Ahmad, A.; Zakaria, Z. Y.; Abdullah, T. A. T.; *Energy*, **2015**, *81*, 255.
13. Guo, J.; Lua, A. C.; *Mater. Lett.*, **2002**, *55*, 334.
14. Guo, J.; Xu, W. S.; Chen, Y. L.; Lua, A. C.; *J. Colloid Interface Sci.*, **2005**, *281*, 285.
15. Kopac, T.; Toprak, A.; *Int. J. Hydrogen Energy*, **2007**, *32*, 5005.
16. Munir, S.; Daood, S. S.; Nimmo, W.; Cunliffe, A. M.; Gibbs, B. M.; *Bioresour. Technol.*, **2009**, *100*, 1413.
17. Luangkiattikhun, P.; Tangsathitkulchai, C.; Tangsathitkulchai, M.; *Bioresour Technol.*, **2008**, *99*, 986.
18. Okoroigwea, E.; Saffronb, DC.; *Nigerian J. Technol.*, **2012**, *31*, 329.
19. Yang, H.; Yan, R.; Chen, H.; Lee, D. H.; Zheng, C.; *Fuel*, **2007**, *86*, 1781.
20. Kim, S. J.; Jung, S. H.; Kim, J. S.; *Bioresour. Technol.*, **2010**, *101*, 9294.
21. Nassar, M. M.; Ashour, E. A.; Wahid, S. S.; *J. Appl. Polym. Sci.*, **1996**, *61*, 885.
22. Skreiberg, A.; Skreiberg, O.; Sandquist, J.; Sørum, L.; *Fuel*, **2011**, *90*, 2182.
23. Gani, A.; Naruse, I.; *Renewable Energy*, **2007**, *32*, 649.
24. Kurniawan, F.; Wongso, M.; Ayucitra, A.; Soetaredjo, F. E.; Angkawijaya, A. E.; Ju, Y. H.; Ismadji, S.; *J. Taiwan Inst. of Chem. Eng.*, **2015**, *47*, 197.
25. Daud, W. M. A. W.; Ali, W. S. W.; Sulaiman, M. Z.; *Carbon*, **2000**, *38*, 1925.
26. Bansal, R. C.; Donnet, J. B.; Stoeckli, F.; Active carbon; Taylor & Francis: United Kingdom, **1988**.
27. Achaw, O. W.; Afrane, G.; *Microporous Mesoporous Mater.*, **2008**, *112*, 284.
28. Gryglewicz, G.; Grabas, K.; Grabowska, E. L.; *Carbon*, **2002**, *40*, 2403.
29. Olutoge, F. A.; Quadri, H. A.; Olafusi, O. S.; *Eng., Technol. Appl. Sci. Research*, **2012**, *2*, 315.
30. Zhou, Q.; Yan, C.; Luo, W.; *Mater. Des.*, **2016**, *97*, 195.
31. Mostaedi M. T.; Asadollahzadeh, M.; Hemmati, A.; Khosravi, A.; *Res. Chem. Intermed.*, **2015**, *41*, 559.
32. Hanafiah, M. A. K. M.; Hussin, Z. M.; Ariff, N. F. M.; Ngah, W. S. W.; Ibrahim, S. C.; *Adv. Mater. Research*, **2014**, *970*, 198.
33. Dorabei, R. Z.; Jalalat, V.; Tadjarodi, A.; *New J. Chem.*, **2016**, *40*, 5128.